Fenretinide derivatives act as disrupters of serum Retinol Binding Protein (sRBP) interactions with Transthyretin (TTR) and the sRBP Receptor

Journal:	*Journal of Medicinal Chemistry*
Manuscript ID:	jm-2011-00256g.R1
Manuscript Type:	Article
Date Submitted by the Author:	12-May-2011

Complete List of Authors:	Campos-Sandoval, José Angel; NUIM, Biology Redondo, Clara; University of Leeds, School of Biochemistry and Molecular Biology Kinsella, Gemma; NUIM, Biology Pal, Akos; NUIM, Biology Jones, Geraint; Sygnature Chemical Services Limited Eyre, Gwen; Sygnature Chemical Services Limited Hirst, Simon; Sygnature Chemical Services Limited Findlay, John; NUI Maynooth, Biology; NUIM, Biology

Fenretinide derivatives act as disrupters of serum Retinol Binding Protein (sRBP) interactions with Transthyretin (TTR) and the sRBP Receptor

José Angel Campos-Sandoval[1], Clara Redondo[2], Gemma K. Kinsella[1], Akos Pal[1], Geraint Jones[3], Gwen S. Eyre[3], Simon C. Hirst[3], John B.C. Findlay[1,2]

[1] The Marie Curie Laboratory for Membrane Proteins, Department of Biology, National University of Ireland, Maynooth, Co. Kildare, Ireland.

[2] School of Biochemistry and Molecular Biology, University of Leeds, Leeds LS2 9JT, U.K.

[3] Sygnature Chemical Services Limited, BioCity, Pennyfoot Street, Nottingham, NG1 1GF, U.K.

Corresponding author: John B.C. Findlay, j.b.c.findlay@leeds.ac.uk, +44(0)113 34 33140; John.Findlay@nuim.ie, +353 1 708 6369.

Abbreviations List:

APC, Allophycocyanin

FEN, Fenretinide

ROH, Retinol

RU, Resonance unit

SDS-PAGE, Sodium dodecyl sulfate polyacrylamide gel electrophoresis

SPR, Surface plasmon resonance

sRBP, Serum retinol-binding protein

TR-FRET, Time-resolved fluorescence resonance energy transfer

TTR, Transthyretin

ABSTRACT

Serum retinol binding protein (sRBP) is released from the liver as a complex with transthyretin (TTR), a process under the control of dietary retinol. Elevated levels of sRBP may be involved in reducing cellular responses to insulin and in generating, first insulin resistance, then type 2 diabetes, offering a new target for therapeutic attack for these conditions.

A series of retinoid analogues were synthesised and examined for their binding to sRBP and their ability to disrupt the sRBP-TTR and sRBP-sRBP receptor interactions. A number inhibit the sRBP-TTR and sRBP-receptor interactions similar to or better than Fenretinide (FEN), presenting a potential novel dual mechanism of action and perhaps offering a new therapeutic intervention against type 2 diabetes and its development. Shortening the chain length of the FEN derivative substantially abolished binding to sRBP, indicating that the strength of the interaction lies in the polyene chain region. Differences in potency against the sRBP-TTR and sRBP-receptor interactions suggest variant effects of the compounds on the two loops of sRBP guarding the entrance of the binding pocket which are responsible for these two protein-protein interactions.

INTRODUCTION

Transport of retinol (ROH, Figure 1) in the blood is controlled by the lipocalin serum retinol binding protein (sRBP, 21 kDa), which is synthesised and released from the liver as a complex with a second protein, transthyretin (TTR).[1-3] sRBP consists of a N terminal coil, eight anti-parallel β strands (A-H) forming a barrel and a short α helix close to the C terminus (PDB: 1RBP[4]).[1] ROH is accommodated in the barrel with the β-ionone ring positioned innermost, the polyene chain fully extended and the hydroxyl end group nearly solvent-exposed near the loops AB, CD and EF (Figure 1). Circulating in the plasma, sRBP is bound to TTR, a homo-tetramer of ~56kDa. Each TTR monomer consists of eight anti-parallel β strands (A-H) arranged similarly to a Greek key β-barrel. One tetramer of TTR can bind two sRBP molecules *in vitro*[5]; however, due to a significant higher concentration of TTR than that of sRBP, each tetramer forms a 1:1 complex in plasma.[6] This association of sRBP-ROH to TTR is believed to prevent its filtration through the kidney glomeruli.[3] In the blood, the uncomplexed or free form of sRBP interacts with a receptor in the plasma membrane of virtually all cells in a ROH-sensitive manner.[7-8] Only the TTR-dissociated holo-sRBP is able to bind to the receptor with high affinity, due to steric hindrance of access to the sRBP:receptor binding site.[7-10] Binding of sRBP to its receptor is followed by the release of retinol and its uptake into the cell via the sRBP receptor.

INSERT FIGURE 1 HERE

A notable paper[11] has chronicled the evidence for an involvement of sRBP in obesity, insulin resistance and type-2 diabetes. sRBP is elevated in insulin resistant mice and humans with obesity and type-2 diabetes.[12] sRBP, is mostly secreted by the liver, but can also come from other tissues, including adipocytes.[13] The source of this excess sRBP is thought to be visceral adipose tissue, hence the link to obesity. sRBP acting on peripheral tissues such as skeletal muscle is postulated to attenuate insulin sensitivity, as indicated by reduced IRS1 phosphorylation and PI3K activity.[11] The mechanism of this proposed effect is unknown but should involve a sRBP-binding entity of some kind.

Fenretinide (4-hydroxy(phenyl)retinamide, FEN, Figure 1) is a synthetic retinoid and has been investigated for potential use in the treatment of cancer, cystic fibrosis, rheumatoid arthritis, acne, psoriasis, and Stargardt's disease. [14-15] Previously, FEN has been shown to compete with retinoids for binding to sRBP (PDB: 1FEL),[16] disrupting sRBP-TTR complexes, and resulting in urinary secretion of sRBP and systemic depletion of ROH.[17] Administration of FEN has been observed to exert therapeutic effects in mouse models of obesity and diabetes.[15] Long-term FEN treatment prevents high-fat diet-induced obesity, insulin resistance, and hepatic steatosis.[18]

The hypothesis we are exploring is that agents which reduce sRBP levels or disrupt the protein interactions that sRBP undergoes, will prevent the genesis of insulin resistance, and consequently that of type 2 diabetes. In this work, we developed a series of retinoid analogues, which were first evaluated experimentally for binding to sRBP through fluorescence measurements. Subsequently, their ability to disrupt protein-protein

interactions was examined through pull-down, time-resolved fluorescence resonance energy transfer (TR-FRET) and surface plasmon resonance (SPR) assays on sRBP-TTR and SPR assays on sRBP with solubilised membranes containing the sRBP:receptor. The later is a novel focus in an effort to determine compounds that exhibit a dual or different effect. Compounds which show differences in their ability to inhibit sRBP:TTR and sRBP:receptor interactions may provide an approach to examining both the validity and the mechanism of action of sRBP levels in the context of insulin resistance and type 2 diabetes.

RESULTS

Retinoid analogues

We were largely interested in establishing if the retinoids could bind to sRBP without necessarily penetrating deep into the binding pocket. We also wished to investigate the level of variability allowed at the region of the molecule near the entrance to the binding cavity – thought to be the effective moiety with regard to alterations in conformation. We were also interested in determining if steric hindrance was the sole and main mechanism for inhibition or a conformational change was also required.

Traditional medicinal chemistry around both ends of a known chemical scaffold (ROH/FEN) was utilized to develop a novel series of retinoid analogues (Figure 2). The target compounds **1-68** were prepared as outlined in Schemes 1-4, see Methods and all chemical structures are shown in the supplementary material.

INSERT FIGURE 2 HERE

The approach of the analysis of these compounds was structured on three levels. The first binding to sRBP was monitored using quenching of the fluorescence of the intrinsic tryptophan in sRBP and/or inhibition of the FRET response of bound retinol. The second involved the sRBP:TTR interaction as monitored by pull-down/SPR responses. The third monitored sRBP:sRBP receptor interactions in solubilized membrane preparations using SPR. Only compounds which provided some evidence for binding to sRBP were progressed to the second and third stages.

Binding of compounds to sRBP

To study the interaction between retinoid analogues and sRBP, the quenching of the intrinsic tryptophan (Trp) fluorescence of the apo-protein following excitation at 280 nm was measured in the presence of increasing concentrations of the compounds. ROH binds to the ligand binding site of the sRBP and produces a quenching of the Trp fluorescence. Those compounds that absorbed in the emission region of Trp reduced this emission in a dose dependent manner, indicative of their specific interaction with the apo-sRBP (Figure 3). The fluorescence intensities of the compounds in a N-acetyl-tryptophanamide solution were measured to correct the titration curves. The change in fluorescence intensities was used to calculate the apparent dissociation constants (K_d) for the protein-compound interactions as described by Cogan *et al.*.[19] The K_d values for selected compounds are shown in Table 1. A K_d of 182±4 nM was obtained for the ROH-sRBP complex, in agreement with that reported in the literature for the protein isolated from human plasma.[19] The other compounds had an affinity in the same range (Table 1).

INSERT FIGURE 3 AND TABLE 1 HERE

Effect of compounds on the sRBP-TTR interaction by pull-down assay

The ability of the 68 library compounds to disrupt the interaction between sRBP and its partner TTR was first examined using a pull-down assay. The purified ROH-sRBP-TTR complex, as indicated in the methods section, was utilized. Both proteins were incubated together in the presence of ROH and the various compounds, at 10 μM and 100 μM, respectively. The difference in concentration between ROH and the compounds allowed for the detection of their inhibitory effect. After incubation with the different compounds, the flow-throughs were run in SDS gels and the free sRBP disrupted from the complexes was detected by silver staining. A representative result for ROH and FEN is shown in Figure 4A. FEN, which is known to disrupt the interaction between sRBP and TTR, was used as a control to which potential positive compounds could be compared. A small quantity of free sRBP was always obtained in the negative control flow-through (no compound added), as a consequence of the relatively weak interaction ($K_d \approx 0.3$ μM) between the two proteins.[21] FEN produced an estimated 3 to 5-fold increase in the amount of sRBP released from the complex. The shorter retinoid analogues, **2**-**22**, which did not exhibit absorption in the Trp emission region, also did not show a disruptive ability of the sRBP-TTR interaction and were disregarded from further studies. A number of compounds based on scaffold B (**1** and **23**-**68**) showed a similar disruptive effect on the complex to FEN. The dose-dependent effect of the positive compounds was similarly assessed using increasing concentrations of the analogues, as shown for one selected compound **58** (Figure 4, panel B).

INSERT FIGURE 4 HERE

sRBP-TTR interaction by TR-FRET

In order to estimate the potency of the different inhibitors selected in the pull-down assay, we continued our analysis of the compounds using a TR-FRET assay based on a methodology developed previously.[22] The sRBP used in this assay was a recombinant protein expressed with a His-tag in *P. pastoris,*[23] to which a europium-labeled anti-His antibody was bound. Native TTR was labeled with biotin. When both proteins bind, and after excitation of europium with light at 340 nm, an energy transfer occurs from europium to streptavidin-conjugated allophycocyanin (APC) and light emission can be detected at 665 nm. A greater signal is observed as the affinity between both proteins increases with ROH concentration. The TR-FRET signal was measured against increasing concentrations of ROH and a constant concentration of inhibitor. The system was tested first with FEN from 0.1 to 50 μM and from this experiment a concentration of 10 μM was selected as appropriate to study the inhibitory effect of the compounds. A set of ROH dose-response curves in the presence of inhibitory compounds is shown in Figure 5. The compounds demonstrated a competitive antagonist effect, as previously shown for FEN,[22] with a shift of the ROH-response curve to the right. FEN produced a 30-fold increase in the EC_{50} (Table 2). Additionally, compound **1** and **58** showed a strong effect, with a 15-fold increase, while the rest of the compounds tested in the TR-FRET assay only produced a slight increase in the EC_{50} (2 to 3-fold).

INSERT FIGURE 5 AND TABLE 2 HERE

sRBP-TTR interaction by Surface Plasmon Resonance

We sought to further expand our understanding of the best retinoid analogues by studying their ability to disrupt the interaction between sRBP and TTR in real time using a surface plasmon resonance (SPR) assay. As shown in Figure 6 the only compound that increases the interaction between sRBP-TTR is ROH, as expected. None of the analogues strengthened the interaction with TTR, but all of them, with the exception of compound **1**, were less disruptive than FEN itself, and hence exhibited qualitatively the same results as with the TR-FRET analysis.

INSERT FIGURE 6 HERE

sRBP-receptor interaction by Surface Plasmon Resonance

The ability of the compounds to disrupt the interaction between sRBP and solubilised membranes was also examined using the SPR binding assay. Detergent-treated HEK293 membrane fractions were pre-incubated with compounds and then injected over sRBP immobilised on the sensorchip surface. All the novel retinoid compounds tested had a negative effect on the stability of the sRBP-membrane protein complex and consequently generated faster dissociation (Figure 7). However, FEN had little or no effect. All experiments were repeated at least three times with no significant differences. Note that background binding to other components of the solubilised membrane will be present.

INSERT FIGURE 7 HERE

DISCUSSION

For some time, there has been great concern about the link between obesity, insulin resistance, type-2 diabetes and cardiovascular disease. A recent scientific discovery provided a way forward towards preventing the avalanche of disability due to type 2 diabetes. This was the observation that elevations in sRBP may attenuate the response of the cell to insulin, thus increasing resistance and presaging type 2 diabetes.[11] A second important element was the much earlier demonstration and functional characterization of a plasma membrane receptor for sRBP[24-25] through which the effects of sRBP might be mediated. The connection with insulin action is a novel one, suggesting a cross-talk between RBP and insulin, since higher levels of the former are seen to dampen down the intracellular response to insulin.[13]

There has been some controversy as to whether sRBP levels are statistically correlated with the development particularly of type 2 diabetes, with reports both confirming[26-29] and failing to confirm the link.[30-32] The reasons for these differences are not clear, the only suggestion put forward so far being some variation in the methodologies used for sRBP estimation.[29] But, very significantly, the first studies on isolated human adipocytes confirmed that elevated sRBP does indeed attenuate insulin-induced IRS-1 and ERKI/2 phosphorylation.[13] Moreover, as was found in the whole animal studies, the serine residue on IRS-1 specifically affected was that closely identified with insulin signalling. Taking this all into account, it seems possible that reducing the “activity” of elevated levels of sRBP may restore normal insulin sensitivity and counteract type 2 diabetes.

The hypothesis we are exploiting is that compounds which reduce sRBP levels, or disrupt its protein interactions will prevent the genesis of insulin resistance, and consequently that of type 2 diabetes and its cardiovascular complications. Administration of FEN has been observed to exert therapeutic effects in mouse models of obesity and diabetes.[15,18] Long-term FEN treatment prevents high-fat diet-induced obesity, insulin resistance, and hepatic steatosis.[18] Additionally, retinoic acid (RA) treatment was determined to reduce body weight, basal serum glucose, serum ROH, and sRBP coupled with improved insulin sensitivity and decreased the ROH-sRBP ratio.[33] In this work, a series of retinoid analogues were synthesized and examined for their ability to disrupt the interaction of sRBP with TTR and, for the first time, with its receptor. As a first step, we measured the binding of these compounds to sRBP by fluorescence titration, a well-established method.[19] The fluorescence emission data was used to calculate K_d values according to the method of Cogan *et al*..[19] The values obtained were consistent with previous work,[19, 34] with a K_d for ROH binding to sRBP of 182±4 nM and comparable values for the analogues **1** and **23** to **68**. This is in agreement with earlier findings, which indicated that modifications of the functional hydroxyl end group of ROH (see Figure 2 and schemes in Methods) do not change substantially the affinity for apo-sRBP.[17, 19, 35] Compounds **2** to **22** did not show any absorption in the Trp emission region and their binding to sRBP could not be assessed by this method. It has been shown that, in order to interact specifically with sRBP, retinoids must possess an intact trymethylcyclohexenyl group that establishes close contacts with the side chains of the internal β-barrel cavity.[35] The lack of a cyclohexene ring or having a shorter structure may limit the binding affinity of

compounds **2**-**22** for sRBP, indicating that the strength of the interaction lies in the polyene chain region.

In the available crystal structures, the ROH hydroxyl group is near the protein surface, in the region of the entrance loops surrounding the opening of the binding cavity. It participates in polar interactions and becomes fully buried in the holo-sRBP–TTR complex.[4] However, the cyclohexene ring and the isoprene tail of FEN take the place of the corresponding portions of ROH, while the hydroxyphenyl amide group protrudes from the cavity toward the solvent, replacing the ROH hydroxyl group and a water molecule hydrogen bonded to it.[16]

Subsequent analysis focused on compounds **1** and **23-68** with an examination of their effect on the interaction between sRBP and TTR. For this purpose, we developed a pull-down assay that could detect free sRBP released from the ROH-sRBP-TTR complex after its disruption in the presence of compounds. The crystal structure of holo-sRBP complexed with TTR revealed that ROH participates in the interaction of sRBP with TTR,[4] increasing the sRBP-TTR affinity 6-fold, from 1.2 μM to 0.3 μM.[21] This relatively low affinity, even for the holo protein, has physiological significance: because holo-sRBP complexed with TTR lacks affinity for its membrane receptor,[9-10] a small amount of uncomplexed holo-sRBP is needed to deliver ROH to the cells through this specific receptor. On the other hand, FEN, with a similar structure to ROH but containing a bulky phenylamide in place of the hydroxyl group, shows a drastic interference with the sRBP-TTR interaction due to steric hindrance in the contact regions between sRBP and TTR and also changes in the position of the loops surrounding the entrance of the binding site.

In agreement with these observations, a low amount of free sRBP was always detected in the control without compounds after incubation of the complex holo-sRBP-TTR in the pull-down assay. In comparison, a higher amount of free sRBP (estimated at 3 to 5-fold) could be measured after incubation of the complex with FEN. Compounds **2-22** did not show a disruptive ability of the sRBP-TTR interaction and were disregarded from further studies. However, a number of compounds based on scaffold B (with variations in the outer end; **1** and **23-68**) showed a similar disruptive effect on the complex to FEN, and probably act through the same mechanism. Interestingly, some of the larger groups at the polyene end of the retinoid analogues extend further than FEN but do not disrupt the sRBP-TTR interaction, indicating that the retinoid analogues may not function solely as steric blockers but perhaps induce conformational changes in the loop regions. This shall be further examined by crystal structure work.

We cannot calculate accurate Ki values because of the nature of the pull-down assay. In all runs (tested at least three times) of this assay, the band intensities were very similar to those for FEN, indicating a disruptive effect with a potency similar to that of FEN. From this qualitative analysis we could draw no definitive conclusions regarding the strength of the disruption of the best analogues and hence additional studies were pursued to validate our initial findings. We used a TR-FRET assay, a technique which has been recently applied to the study of sRBP-TTR interactions, to characterize their inhibitory behaviour.[22] The selected compounds produced a decrease in the basal interaction between sRBP and TTR in the absence of ROH, and a right shift of the ROH curve compared to the control (no compound). This is in agreement with the competitive behaviour described for FEN and retinyl acetate.[22] The TR-FRET results were also

validated using a secondary binding assay, SPR, which yielded qualitatively similar results, with FEN and compound **1** exhibiting a more disruptive sRBP-TTR effect while the other compounds were clustered together in both assays.

With the SPR assay using the HEK293-cell membranes and immobilised His-sRBP, ROH had a positive effect on the interaction observed in real time and the compounds all had a disruptive effect, with FEN exhibiting the smallest disruption of the set. We have shown values for the disruption of the RBP-TTR interaction from FRET assays but it is not possible to generate other than relative potencies for the sRBP-receptor interactions because of the nature of SPR with solubilised whole membrane preparations. The usual problem is that accurate values can only be obtained when pure preparations of a receptor are used.

Using our three tiered assay approach, including analysing binding to sRBP and SPR studies on the sRBP:TTR and sRBP:sRBP receptor interaction, we were able to show that most sRBP binders exhibited a dual effect. Some compounds inhibited TTR more than the receptor interaction; a few the reverse. It is known that FEN reduces sRBP levels and improves insulin sensitivity,[11,16,36] probably by disrupting the ROH-sRBP-TTR complex promoting clearance of sRBP.[11,17] Our SPR data suggest that FEN might have a dual-effect on the RBP insulin resistance link, by i) lowering sRBP levels, and ii) interacting directly with the insulin pathway inside the cell, its uptake having been mediated by the sRBP receptor. This is supported by the observation that FEN only "mildly" interferes with the interaction of sRBP-ROH with membrane compared to the strong disruption of that interaction caused by other compounds.

CONCLUSIONS

In this work, a number of active retinoid-like molecules have been determined that inhibit sRBP-TTR and sRBP-receptor interactions similar to or better than FEN, the anti-tumour positive control, thereby presenting a potential novel dual mechanism of action. Thus, the compounds discovered may offer a new therapeutic intervention against type 2 diabetes and its development.

EXPERIMENTAL:

BIOLOGY EXPERIMENTAL

Materials

BL21(DE3) *Escherichia coli* strain, *Pichia pastoris* strain KM71H (*aox1::ARG4, arg4*), expression vector pPICZ-α A, Zero Blunt TOPO PCR cloning kit and europium-labeled anti-His-tag antibodies were purchased from Invitrogen. HEK293293 cells (human embryonic kidney) were from the ATCC. SureLight streptavidin-conjugated allophycocyanin (APC) was from PerkinElmer. EZ-Link Sulfo-NHS-LC-Biotinylation kit was from Pierce. ROH, FEN, native human TTR and synthetic oligonucleotide primers were from Sigma. PCR amplification of coding sequences was performed with PfuTurbo Hotstart DNA polymerase from Stratagene. Ni-NTA superflow resin and cobalt affinity gel were purchased from Qiagen and Sigma, respectively. Plasmid isolation and gel extraction kits were from Qiagen. Biacore materials were obtained from GE Healthcare. Retinoid analogues were synthesised by Sygnature Chemical Services. Other reagents used were molecular biology grade.

Expression and purification of recombinant human sRBP in E. coli

The mature form of human sRBP was expressed without tags using the vector pMMHa. NdeI and BamHI restriction sites flanking the coding sequence of mature human sRBP (corresponding to residues 19-201) were constructed by PCR using the sRBP cDNA originally cloned into the pQE-30 vector.[9] The oligonucleotide primers designated to amplify the insert were NdeI (forward) 5´-TACATATGGAGCGCGACTGCCGAGTG-

3´ and BamHI (reverse) 5´-TAGGATCCCTACAAAAGGTTTCTTTCTGATCTGC-3´. The PCR product was inserted into the pCR-Blunt II TOPO vector, digested with NdeI and BamHI and introduced into the same restriction sites of the pMMHa vector under the control of T7 promoter.

BL21(DE3) cells transformed with the expression plasmid pMMHa-sRBP were grown in 2×YT medium (1.6 % tryptone, 1 % yeast extract, 0.5 % NaCl) with 100 μg/mL ampicillin. When the cell culture reached an optical density of 0.6 at 600 nm, protein expression was induced by 1mM IPTG. After overnight incubation at 37°C, the cells were harvested by centrifugation at 7000 g for 10 min at 4°C and subjected to disruption by sonication. The resulting suspension was centrifuged at 10000 g for 10 min at 4°C and the pellet (sRBP inclusion bodies) suspended at 1 mg/mL of sRBP in 5 M guanidinium chloride with 10 mM DTT at a pH of 9.0 to help in reduction and solubilisation of recombinant protein. After overnight incubation at 25°C, the refolding of sRBP was started by dilution of the denatured protein to a concentration of 0.25 mg/mL in cold refolding buffer (25 mM Tris-HCl pH 9.0, 0.3 mM cystine, 3 mM cysteine, 1 mM EDTA) with 10-fold molar excess of ROH.[37] The guanidinium chloride concentration at this step was 1 M. After refolding, the protein solution was dialysed against PBS buffer and then refolded sRBP was purified by affinity chromatography with His-TTR (see below).

Expression and purification of recombinant human sRBP in P. pastoris

The sRBP was expressed with a N-terminal His-tag using the *P. pastoris* expression system as described previously.[23] The sRBP coding sequence was amplified by PCR

using the oligonucleotide primers EcoRI (forward) 5´-GAATTCCATCATCATCATCATCATGAGCGCGACTGCCGAGTG-3´and XbaI (reverse) 5´-TCTAGACTACAAAAGGTTTCTTTCTGATCTGCC-3´. The forward primer included the sequence for a 6×His-tag. The PCR product was ligated in the pCR-Blunt II TOPO vector and subsequently introduced into the EcoRI/XbaI sites of pPICZα A vector under the control of the AOX1 promoter.

P. pastoris cells were transformed with the expression vector pPICZα A-His-sRBP and grown at 30°C in phosphate-buffered YP medium (1% yeast extract, 2% peptone, pH 7.5) in the presence of 2% glycerol (w/v) until the OD_{600} was 6.0. The cells were harvested by centrifugation at 7000 g for 10 min and used to inoculate YP medium to an OD_{600} of 1.0 supplemented with 1% methanol (v/v) to induce expression. For each of 2 days, methanol was added to a final concentration of 1% (v/v). After 48 h of induction, the culture supernatant containing the His-sRBP was incubated with Ni-NTA resin and the bound proteins eluted with elution buffer (20 mM Na_2HPO_4, 500 mM NaCl, 250 mM imidazole, pH 7.4). The purified His-sRBP was dialysed against PBS buffer and then concentrated by ultrafiltration.

Expression and purification of recombinant human His-TTR

The coding sequence of human TTR in the vector pMMHa was a gift of Dr. J.W. Kelly.[38] In order to facilitate the subsequent purification of the holo-sRBP-TTR complex, TTR was expressed with a N-terminal His-tag. The coding sequence of mature TTR (corresponding to residues 21-147) was inserted into the BamHI and HindIII restriction sites in the pQE-30 vector. The oligonucleotide primers used in the PCR were BamHI

(forward) 5´-GGATTCGGCCCTACGGGCACCG-3´and HindIII (reverse) 5´-AAGCTTTCATTCCTTGGGATTGGTGACG-3´. The PCR product was ligated in the pCR-Blunt II TOPO vector, digested with BamHI and HindIII and inserted into the pQE-30 vector.

The expression of this protein in *E. coli* was performed as for sRBP. After overnight induction with IPTG, the cells were collected and sonicated. The supernatant containing the soluble TTR was incubated with Ni-NTA resin and the recombinant protein eluted with elution buffer. The purified His-TTR was dialysed against PBS buffer.

Purification of ROH-sRBP-TTR complex

Purified His-TTR was added to the refolded, untagged holo-sRBP solution and incubated overnight at 4°C in the presence of 100 μM ROH. Then, the protein solution was applied to a cobalt affinity column equilibrated with buffer I (20 mM Na_2HPO_4, 500 mM NaCl, 10 mM imidazole, pH 7.4). The column was washed with the same buffer and then eluted with elution buffer. Fractions were analysed by SDS-PAGE and Coomassie staining.

Fluorimetric binding assays

The binding of compounds to His-sRBP was monitored by titration of the intrinsic fluorescence emission of the protein in the presence of increasing concentrations of compounds. The quenching of protein fluorescence due to energy transfer to the ligand was evaluated using excitation and emission wavelengths of 280 and 350 nm, respectively, in a Cary Eclipse fluorescence spectrophotometer (Varian). Purified His-sRBP expressed with the *P. pastoris* system was diluted to a concentration of 2 μM in

PBS buffer and small increments of compounds solutions in ethanol were added. The system was mixed and allowed to equilibrate for 5 min before recording the fluorescence emission of the compound-His-sRBP complex. The final concentration of ethanol never exceeded 2 %. A solution of N-acetyl-L- tryptophanamide was used as a blank. The apparent dissociation constants (K_d) of compounds from His-sRBP were estimated as described by Cogan *et al.*. [19]

sRBP-TTR interaction by pull-down assay

The capacity of the compounds that bind to sRBP to disrupt the interaction between this protein and its partner TTR was examined first by a pull-down assay. In this assay, the purified holo-sRBP-TTR complex (0.2 mg/mL in PBS buffer pH 7.4) was incubated in the presence of 10 µM Retinol and 100 µM of each compound, for 1 h at 37°C. Then, 20 µL of Cobalt resin were added to separate by pull-down the fraction of free sRBP from the fraction bound to TTR. The flow-throughs, containing the free sRBP, were examined by SDS-PAGE and silver staining. A control with FEN, which is known to disrupt the interaction between sRBP and TTR, was included in the assay for comparison.

Time-resolved FRET

The TR-FRET assay was based on a previously published protocol by Coward *et al.*.[22] The reactions were prepared in white 96-well plates (Greiner) in a final volume of 100 µL. Native TTR was biotinylated according to the manufacturer´s manual. Each well contained 5 nM apo-His-sRBP, 100 nM biotinylated-TTR, 100 nM SureLight streptavidin-conjugated APC, 1 nM europium-labeled anti-His-tag antibody, 10 µM of

inhibitor and increasing concentrations of ROH in TR-FRET buffer (20 mM Tris-HCl pH 7.4, 150 mM NaCl, 1 mM EDTA, 0.01 % BSA, 0.02 % Tween-20). Reactions were incubated for 2 h at room temperature and measured on a POLARstar Omega microplate reader (excitation wavelength 337 nm, emission wavelengths 615 and 665 nm).

Surface Plasmon Resonance (SPR)

Interaction analyses were performed in SPR running buffer (HBS with 50µM EDTA) at a flow rate of 10µl/min, at constant temperature (25^0C), using a Biacore 3000 system (GE Healthcare). Ni-NTA sensor chips were used for all experiments and general procedures were performed according to the manufacturer's instructions for this sensor chip. Briefly, each cycle consisted of: surface activation with 20µl of nickel (2 min), followed by a 5 min injection of recombinant sRBP (His-tagged, 200 nM solution, prepared in SPR running buffer), and followed by a 1 min pulse of a specific concentration of compound (diluted in SPR running buffer), culminating with (i) a 5 min injection of untagged, native TTR (1 µM in running buffer incubated with 10 µM each compound), or (ii) a 5 min injection of solubilised HEK293 cells membranes[9] (50µg/ml in running buffer incubated with 10 µM of each compound); finally sensor chip regeneration was achieved by stripping all proteins from the surface, performing a 2 min injection of 0.3 mM EDTA in HBS, at the end of each cycle (max. number of regenerations/chip: n=100). Sensor chips were used for 2 weeks, or until nonspecific binding increased (>= 5%). All experiments were performed in parallel with an inactivated flow cell not coated with protein. Each independent experiment was repeated 3-5 times.

Data Processing

Prism 5.00 (GraphPad Software Inc.) was used to determine EC_{50} values. All SPR sensorgrams were corrected for buffer induced refractive index changes at an uncoated reference surface, analysed using BIAEVALUATION software (BIAEVAL 3.2, GE Healthcare).

CHEMISTRY EXPERIMENTAL

For compound purity determination, the system consisted of a Waters HPLC and mass spectrometer system and an Agilent Scalar 5 μm C18 50 x 4.6 mm column. Detection was achieved using an electrospray ionization source (positive or negative ion), a UV detector at 254 nm and 215 nm. Mobile Phase A: 0.1% aqueous formic acid, Mobile Phase B: 0.1% formic acid in MeCN. Flow rate 2.5 mL/min: Gradient: 0-0.1 min 5% B; 0.1-5min 5-95%B; 5-5.5min 95% B; 5.5-5.6 min 95% B, flow increased to 3.5 mL/min; 5.6-6.6 95% B; 6.6-6.75 min 95-5% B; 6.75-6.9 min 5% B; 6.9-7 min 5% B, flow reduced to 2.5 mL/min. The majority of the library supplied was > 95% pure.

Scheme 1:

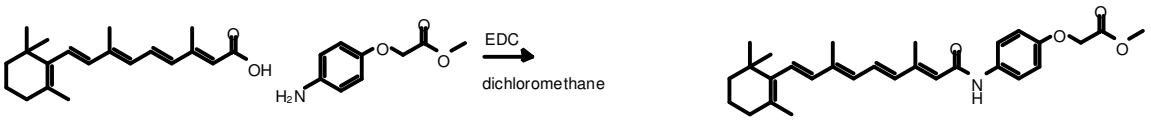

Preparation:

Retinoic acid (1 g, 3.33 mmol) and EDC (0.957 g, 4.99 mmol) were stirred in DCM (20ml) and methyl 2-(4-aminophenoxy)acetate (0.724 g, 3.99 mmol) was added. After 16 hr the reaction mixture was applied to a silica cartridge (80 g) and eluted with EtOAc/isohexane (1:3 v/v) to afford the target compound as a yellow oil which solidifies on standing.

1, methyl 2-(4-((2*E*,4*E*,6*E*,8*E*)-3,7-dimethyl-9-(2,6,6-trimethylcyclohex-1-en-1-yl)nona-2,4,6,8-tetraenamido)phenoxy)acetate: R^t 3.02 min; m/z 464 $(M+H)^+$, (ES^+); Yield 0.5226 g, 34 %. Purity; 100%.

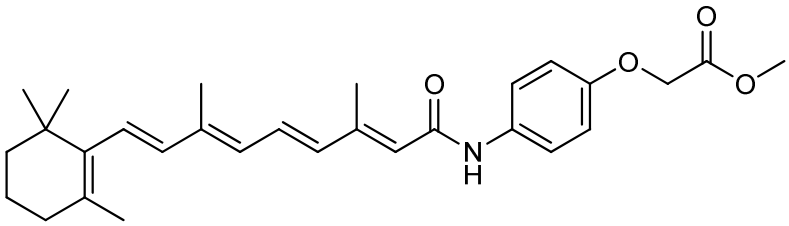

Scheme 2:

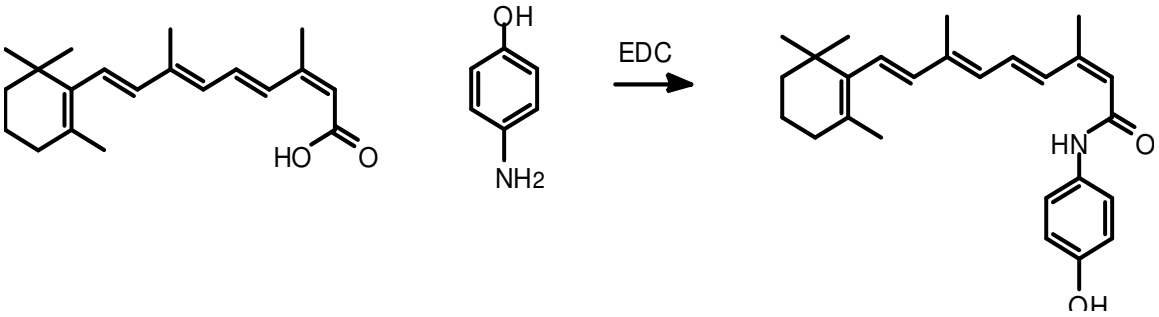

Preparation:

4-Hydroxyaniline (43.6 mg, 0.399 mmol) was added to a solution of cis-Retinoic acid (100 mg, 0.333 mmol) and EDC (96 mg, 0.499 mmol) in DCM (1ml) and the reaction stirred at room temperature overnight.

Reaction was diluted with water and passed through a phase separator. The organic layer was applied to a 4g silica cartridge and eluted with 0-100% EtOAc in cyclohexane. This gave a yellow solid.

23, (2*Z*,4*E*,6*E*,8*E*)-*N*-(4-hydroxyphenyl)-3,7-dimethyl-9-(2,6,6-trimethylcyclohex-1-en-1-yl)nona-2,4,6,8-tetraenamide: R^t 2.82 min; m/z 392 $(M+H)^+$, (ES^+); Yield; 13.6 mg, 10%. Purity; 94%.

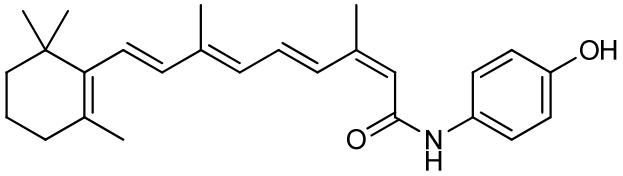

Scheme 3

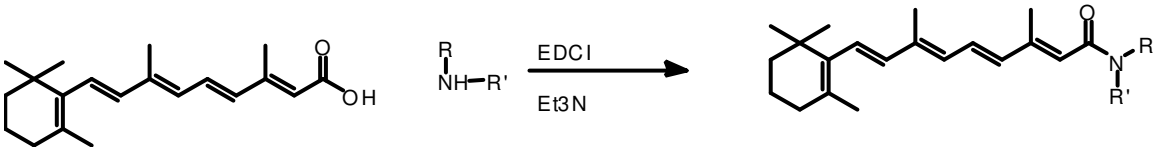

Preparation:

Amine (0.4 mmol, 1.2 eq) was added to Retinoic acid (100 mg, 0.333 mmol), EDCI (96 mg, 0.499 mmol) in DCM (1ml). The reactions were then stirred at rt for 24 hours. All reactions were investigated by LCMS. Those showing desired product were quenched with water and the mixture passed through a phase separator. Products were purified by prep HPLC.

41, (2E,4E,6E,8E)-N-(2,3-dihydroxypropyl)-3,7-dimethyl-9-(2,6,6-trimethylcyclohex-1-en-1-yl)nona-2,4,6,8-tetraenamide: R^t 4.72 min; m/z 374 $(M+H)^+$, (ES^+); Yield 7.8 mg, 6%. Purity; 92%.

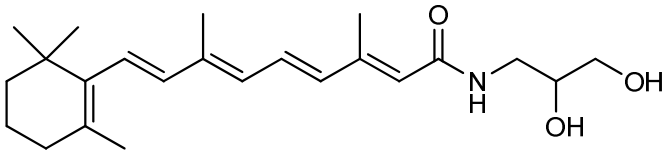

48, (2E,4E,6E,8E)-N-(2-hydroxyethyl)-3,7-dimethyl-9-(2,6,6-trimethylcyclohex-1-en-1-yl)nona-2,4,6,8-tetraenamide: R^t 2.60 min; m/z 344 $(M+H)^+$, (ES^+); Yield 12.2 mg, 11%. Purity; 90%.

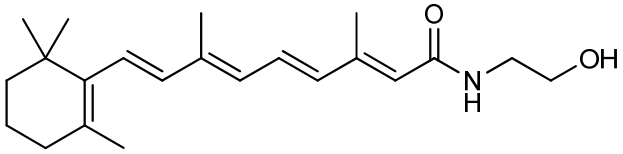

Scheme 4:

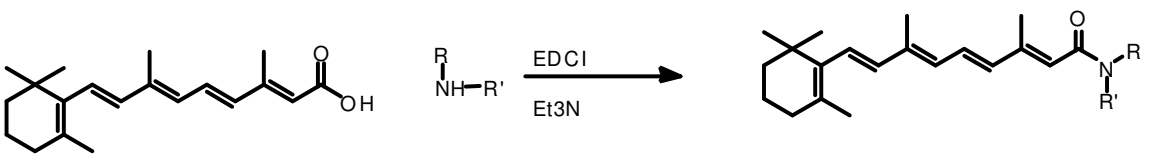

Amine (0.4 mmol, 1.2 eq) was added to Retinoic acid (100 mg, 0.333 mmol), and EDCI (96 mg, 0.499 mmol) in DCM (1ml). The reactions were then stirred at rt for 24 hours. All reactions were investigated by LCMS. Those showing desired product were quenched with water and the mixture passed through a phase separator.

All products were purified on 4g silica cartridges eluting with 0-100% (5% MeOH in EtOAc) in isohexane.

58, (2*E*,4*E*,6*E*,8*E*)-N-(4-(dimethylamino)phenyl)-3,7-dimethyl-9-(2,6,6-trimethylcyclohex-1-en-1-yl)nona-2,4,6,8-tetraenamide: R^t 3.22 min; m/z 419 $(M+H)^+$, (ES^+); Yield 15.3 mg, 11%. Purity; 91%.

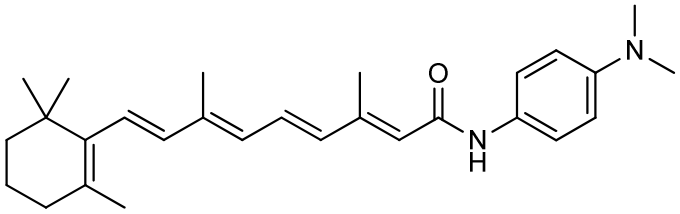

62, (2*E*,4*E*,6*E*,8*E*)-3,7-dimethyl-1-morpholino-9-(2,6,6-trimethylcyclohex-1-en-1-yl)nona-2,4,6,8-tetraen-1-one: R^t 3.09 min; m/z 370 $(M+H)^+$, (ES^+); Yield 10.8 mg, 9%. Purity; 98%.

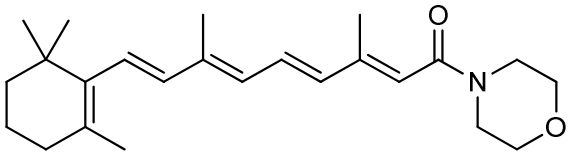

ACKNOWLEDGMENTS

This work was supported by the Marie Curie Transfer of Knowledge Scheme (MTKD-CT-2006-042480) and an Enterprise Ireland proof of concept (POC) grant (PC-2007-047**).** G.K.K. acknowledges the support of an Irish Research Council for Science, Engineering and Technology (IRCSET) postdoctoral fellowship, PD-2008-28.

The authors wish to acknowledge the SFI/HEA Irish Centre for High-End Computing (ICHEC), the NUIM HPC centre and the HEA Trinity Centre for High Performance Computing (TCHPC) for the provision of computational facilities and support. The authors sincerely thank the software vendors for their continuing support for such academic research efforts, in particular contributions from Openeye Scientific, Scitegic and the Chemical Computing Group.

Supporting Information Availability:

Chemical structures of compounds **1-68** are given in the supplementary material. This material is available free of charge via the internet at http://pubs.acs.org.

REFERENCES

1. Zanotti, G.; Folli, C.; Cendron, L.; Alfieri, B.; Nishida, S.; Gliubich, F.; Pasquato, N.; Negro, A.; Berni, R. Structural and mutational analyses of protein-protein interactions between transthyretin and retinol-binding protein. *FEBS J* 2008, 275, 5841-5854.

2. Kanai, M.; Raz, A.; Goodman, D. Retinol-binding protein: the transport protein for vitamin A in human plasma. *J Clin Invest* 1968, 47, 2025-2044.

3. Wolf, G. Multiple functions of vitamin A. *Physiol Rev* 1984, 64, 873-937.

4. Cowan, S.; Newcomer, M.; Jones, T. Crystallographic refinement of human serum retinol binding protein at 2A resolution. *Proteins* 1990, 8, 44-61.

5. Monaco, H.; Rizzi, M.; Coda, A. Structure of a complex of two plasma proteins: transthyretin and retinol-binding protein. *Science* 1995, 268, 1039-1041.

6. Goodman, D. Overview of current knowledge of metabolism of vitamin A and carotenoids. *J Natl Cancer Inst* 1984, 73, 1375-1379.

7. Kawaguchi, R.; Yu, J.; Honda, J.; Hu, J.; Whitelegge, J.; Ping, P.; Wiita, P.; Bok, D.; Sun, H. A membrane receptor for retinol binding protein mediates cellular uptake of vitamin A. *Science* 2007, 315, 820-825.

8. Kawaguchi, R.; Yu, J.; Wiita, P.; Honda, J.; Sun, H. An essential ligand-binding domain in the membrane receptor for retinol-binding protein revealed by large-scale mutagenesis and a human polymorphism. *J Biol Chem* 2008, 283, 15160-15168.

9. Redondo, C.; Vouropoulou, M.; Evans, J.; Findlay, J. Identification of the retinol-binding protein (RBP) interaction site and functional state of RBPs for the membrane receptor. ***FASEB J*** **2008, 22, 1043-1054.**

10. Sivaprasadarao, A.; Sundaram, M.; Findlay, J. Interactions of retinol-binding protein with transthyretin and its receptor. ***Methods Mol Biol*** **1998, 89, 155-163.**

11. Yang, Q.; Graham, T.; Mody, N.; Preitner, F.; Peroni, O.; Zabolotny, J.; Kotani, K.; Quadro, L.; Kahn, B. Serum retinol binding protein 4 contributes to insulin resistance in obesity and type 2 diabetes. ***Nature*** **2005, 436, 356-362.**

12. Graham, T.; Yang, Q.; Blüher, M.; Hammarstedt, A.; Ciaraldi, T.; Henry, R.; Wason, C.; Oberbach, A.; Jansson, P.; Smith, U.; Kahn, B. Retinol-binding protein 4 and insulin resistance in lean, obese, and diabetic subjects. ***N Engl J Med*** **2006, 354, 2552-2563.**

13. Ost, A.; Danielsson, A.; Lidén, M.; Eriksson, U.; Nystrom, F.; Strålfors, P. Retinol-binding protein-4 attenuates insulin-induced phosphorylation of IRS1 and ERK1/2 in primary human adipocytes. ***FASEB J*** **2007, 21, 3696-3704.**

14. Zanardi, S.; Serrano, D.; Argusti, A.; Barile, M.; Puntoni, M.; Decensi, A. Clinical trials with retinoids for breast cancer chemoprevention. ***Endocr Relat Cancer*** **2006, 13, 51-68.**

15. Radu, R.; Han, Y.; Bui, T.; Nusinowitz, S.; Bok, D.; Lichter, J.; Widder, K.; Travis, G.; Mata, N. Reductions in serum vitamin A arrest accumulation of toxic retinal fluorophores: a potential therapy for treatment of lipofuscin-based retinal diseases. ***Invest Ophthalmol Vis Sci*** **2005, 46, 4393-4401.**

16. Zanotti, G.; Marcello, M.; Malpeli, G.; Folli, C.; Sartori, G.; Berni, R. Crystallographic studies on complexes between retinoids and plasma retinol-binding protein. ***J Biol Chem*** **1994, 269, 29613-29620.**

17. Berni, R.; Formelli, F. In vitro interaction of fenretinide with plasma retinol-binding protein and its functional consequences. ***FEBS Lett*** **1992, 308, 43-45.**

18. Preitner, F.; Mody, N.; Graham, T.; Peroni, O.; Kahn, B. Long-term Fenretinide treatment prevents high-fat diet-induced obesity, insulin resistance, and hepatic steatosis. ***Am J Physiol Endocrinol Metab*** **2009, 297, E1420-9.**

19. Cogan, U.; Kopelman, M.; Mokady, S.; Shinitzky, M. Binding affinities of retinol and related compounds to retinol binding proteins. ***Eur J Biochem*** **1976, 65, 71-78.**

20. MOE Chemical Computing Group, N. In MOE Chemical Computing Group, Nov. 2008.

21. Malpeli, G.; Folli, C.; Berni, R. Retinoid binding to retinol-binding protein and the interference with the interaction with transthyretin. ***Biochim Biophys Acta*** **1996, 1294, 48-54.**

22. Coward, P.; Conn, M.; Tang, J.; Xiong, F.; Menjares, A.; Reagan, J. Application of an allosteric model to describe the interactions among retinol binding protein 4, transthyretin, and small molecule retinol binding protein 4 ligands. ***Anal Biochem*** **2009, 384, 312-320.**

23. Wysocka-Kapcinska, M.; Campos-Sandoval, J.; Pal, A.; Findlay, J. Expression and characterization of recombinant human retinol-binding protein in Pichia pastoris. ***Protein Expr Purif*** **2010, 71, 28-32.**

24. Redondo, C.; Burke, B.; Findlay, J. The retinol-binding protein system: a potential paradigm for steroid-binding globulins? *Horm Metab Res* 2006, 38, 269-278.

25. Sivaprasadarao, A.; Findlay, J. The interaction of retinol-binding protein with its plasma-membrane receptor. *Biochem J* 1988, 255, 561-569.

26. Cho, Y.; Youn, B.; Lee, H.; Lee, N.; Min, S.; Kwak, S.; Lee, H.; Park, K. Plasma retinol-binding protein-4 concentrations are elevated in human subjects with impaired glucose tolerance and type 2 diabetes. *Diabetes Care* 2006, 29, 2457-2461.

27. Craig, R.; Chu, W.; Elbein, S. Retinol binding protein 4 as a candidate gene for type 2 diabetes and prediabetic intermediate traits. *Mol Genet Metab* 2007, 90, 338-344.

28. Gavi, S.; Stuart, L.; Kelly, P.; Melendez, M.; Mynarcik, D.; Gelato, M.; McNurlan, M. Retinol-binding protein 4 is associated with insulin resistance and body fat distribution in nonobese subjects without type 2 diabetes. *J Clin Endocrinol Metab* 2007, 92, 1886-1890.

29. Graham, T.; Wason, C.; Blüher, M.; Kahn, B. Shortcomings in methodology complicate measurements of serum retinol binding protein (RBP4) in insulin-resistant human subjects. *Diabetologia* 2007, 50, 814-823.

30. Lee, D.; Lee, J.; Im, J. Association of serum retinol binding protein 4 and insulin resistance in apparently healthy adolescents. *Metabolism* 2007, 56, 327-231.

31. Janke, J.; Engeli, S.; Boschmann, M.; Adams, F.; Böhnke, J.; Luft, F.; Sharma, A.; Jordan, J. Retinol-binding protein 4 in human obesity. *Diabetes* 2006, 55, 2805-2810.

32. Takashima, N.; Tomoike, H.; Iwai, N. Retinol-binding protein 4 and insulin resistance. *N Engl J Med* 2006, 355, 1392; author reply 1394-1395.

33. Manolescu, D.; Sima, A.; Bhat, P. All-trans retinoic acid lowers serum retinol-binding protein 4 concentrations and increases insulin sensitivity in diabetic mice. *J Nutr* 2010, 140, 311-316.

34. Noy, N.; Xu, Z. Interactions of retinol with binding proteins: implications for the mechanism of uptake by cells. *Biochemistry* 1990, 29, 3878-3883.

35. Berni, R.; Clerici, M.; Malpeli, G.; Cleris, L.; Formelli, F. Retinoids: in vitro interaction with retinol-binding protein and influence on plasma retinol. *FASEB J* 1993, 7, 1179-1184.

36. Johansson, H.; Gandini, S.; Guerrieri-Gonzaga, A.; Iodice, S.; Ruscica, M.; Bonanni, B.; Gulisano, M.; Magni, P.; Formelli, F.; Decensi, A. Effect of fenretinide and low-dose tamoxifen on insulin sensitivity in premenopausal women at high risk for breast cancer. *Cancer Res* 2008, 68, 9512-9518.

37. Xie, Y.; Lashuel, H.; Miroy, G.; Dikler, S.; Kelly, J. Recombinant human retinol-binding protein refolding, native disulfide formation, and characterization. *Protein Expr Purif* 1998, 14, 31-37.

38. Lashuel, H.; Wurth, C.; Woo, L.; Kelly, J. The most pathogenic transthyretin variant, L55P, forms amyloid fibrils under acidic conditions and protofilaments under physiological conditions. *Biochemistry* 1999, 38, 13560-13573.

39. DeLano WL., D. S. *The PyMOL Molecular Graphics System.*, Palo Alto, CA, USA, 2002.

TABLE LEGENDS

Table 1: Apparent dissociation constants (K_d) for the protein-compounds interactions calculated according to the method of Cogan *et al.*.[19] Data shown are average values ± standard deviation (SD) from three independent experiments.

Compound	Structure	Kd (nM)	SD
ROH	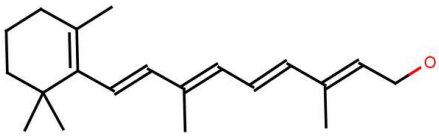 (all-E)-3,7-Dimethyl-9-(2,6,6-trimethyl-1 cyclohexen-1-yl)-2,4,6,8-nonatetraen-1-ol	182	4
FEN	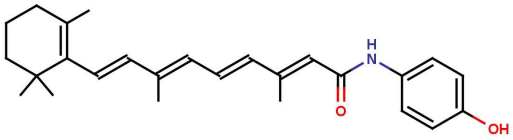 (2E,4E,6E,8E)-N-(4-hydroxyphenyl)-3,7-dimethyl-9-(2,6,6-trimethylcyclohex-1-en-1-yl)nona-2,4,6,8-tetraenamide	156	18
1	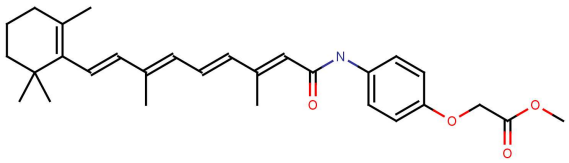 methyl 2-{4-[(2E,4E,6E,8E)-3,7-dimethyl-9-(2,6,6-trimethylcyclohex-1-en-1-yl)nona-2,4,6,8-tetraenamido]phenoxy}acetate	131	43

23	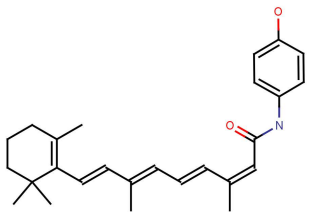 (2Z,4E,6E,8E)-N-(4-hydroxyphenyl)-3,7-dimethyl-9-(2,6,6-trimethylcyclohex-1-en-1-yl)nona-2,4,6,8-tetraenamide	333	24
41	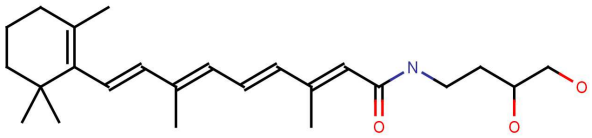 (2E,4E,6E,8E)-N-(2,3-dihydroxypropyl)-3,7-dimethyl-9-(2,6,6-trimethylcyclohex-1-en-1-yl)nona-2,4,6,8-tetraenamide	178	20
48	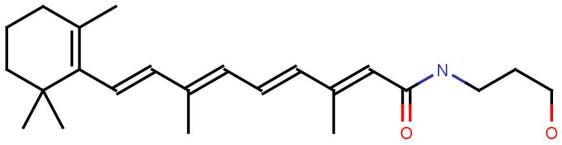 (2E,4E,6E,8E)-N-(2-hydroxyethyl)-3,7-dimethyl-9-(2,6,6-trimethylcyclohex-1-en-1-yl)nona-2,4,6,8-tetraenamide	214	32
58	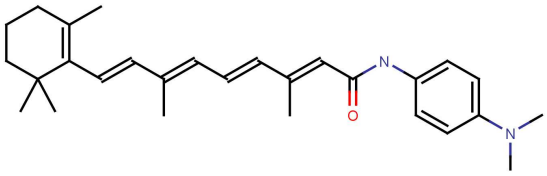 (2E,4E,6E,8E)-N-[4-(dimethylamino)phenyl]-3,7-dimethyl-9-(2,6,6-trimethylcyclohex-1-en-1-yl)nona-2,4,6,8-tetraenamide	98	21

62	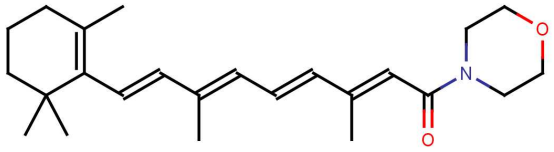 (2E,4E,6E,8E)-3,7-dimethyl-1-(morpholin-4-yl)-9-(2,6,6-trimethylcyclohex-1-en-1-yl)nona-2,4,6,8-tetraen-1-one	227	35

Table 2: EC_{50} values for ROH-sRBP-TTR interaction in the presence of compounds. Data shown are average values ± standard deviation (SD) from three independent experiments.

Compound	EC_{50} (nM)	SD
no compound	71	11
Fenretinide	2372	186
1	1260	177
23	245	35
41	171	21
48	145	5
58	954	114
62	154	17

FIGURES

Figure 1

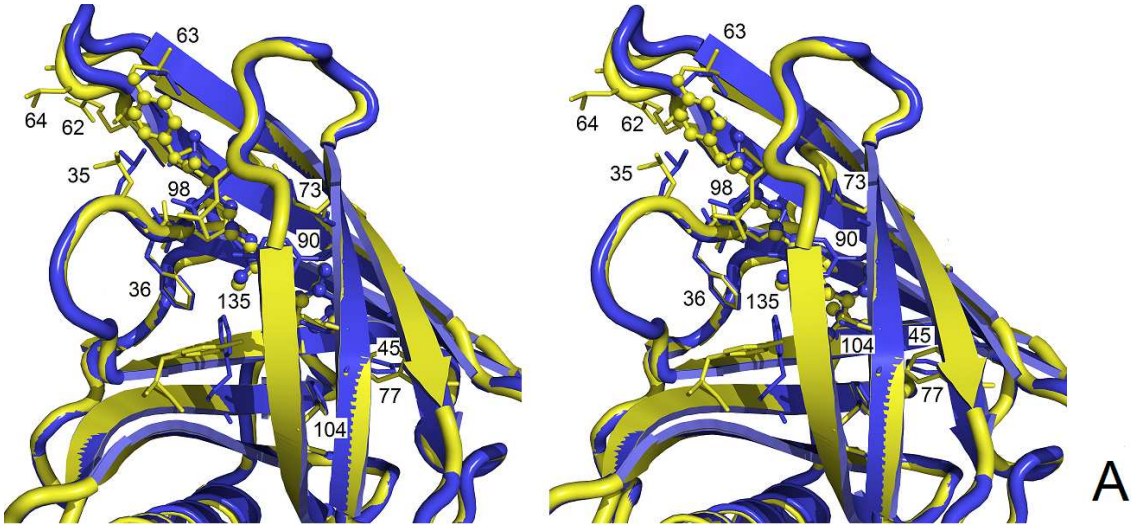

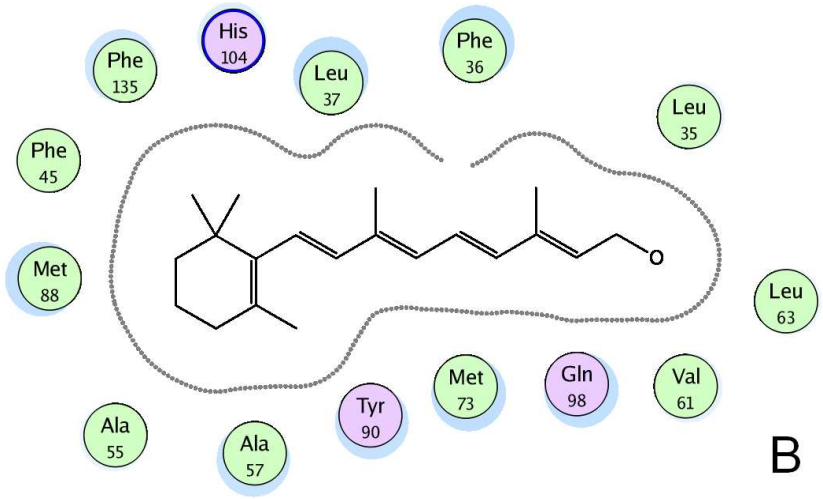

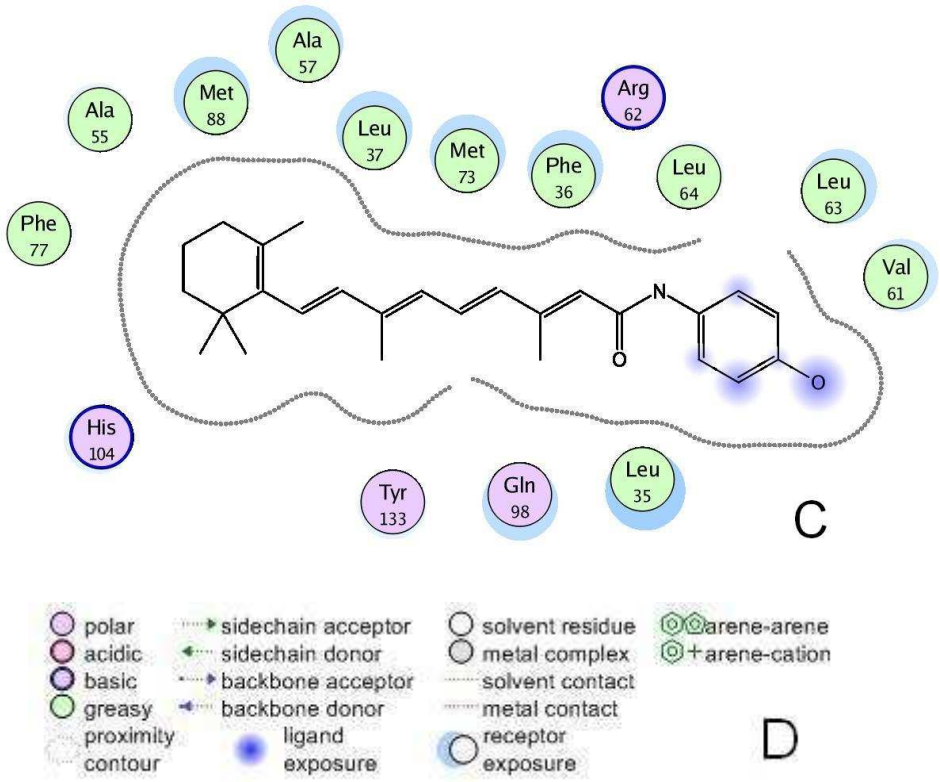
Ala 57
Met 88
Ala 55
Leu 37
Met 73
Arg 62
Phe 36
Leu 64
Leu 63
Phe 77
Val 61
N
O
O
His 104
Tyr 133
Gln 98
Leu 35
C

polar
acidic
basic
greasy
proximity
contour
sidechain acceptor
sidechain donor
backbone acceptor
backbone donor
ligand exposure
solvent residue
metal complex
solvent contact
metal contact
receptor exposure
arene-arene
arene-cation
D

Figure 2

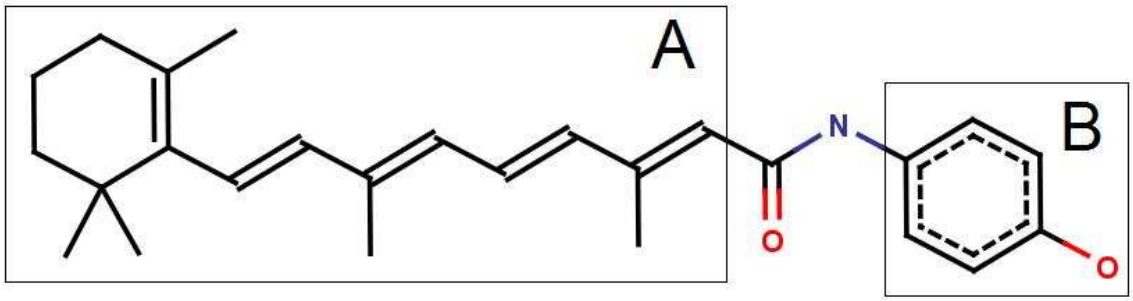

Figure 3

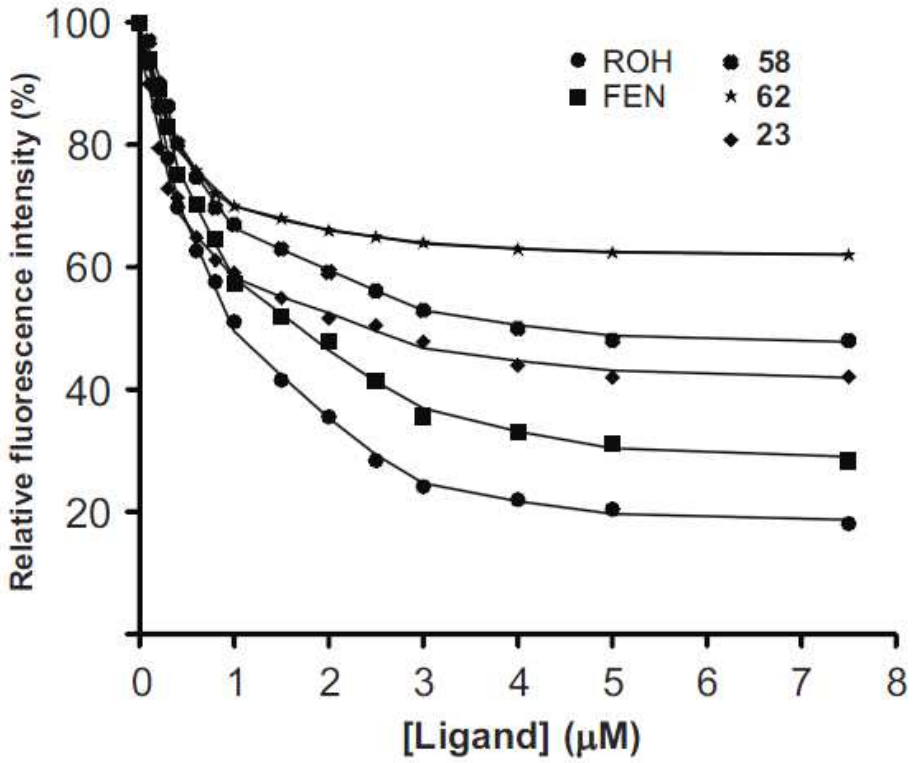

Figure 3

Figure 4

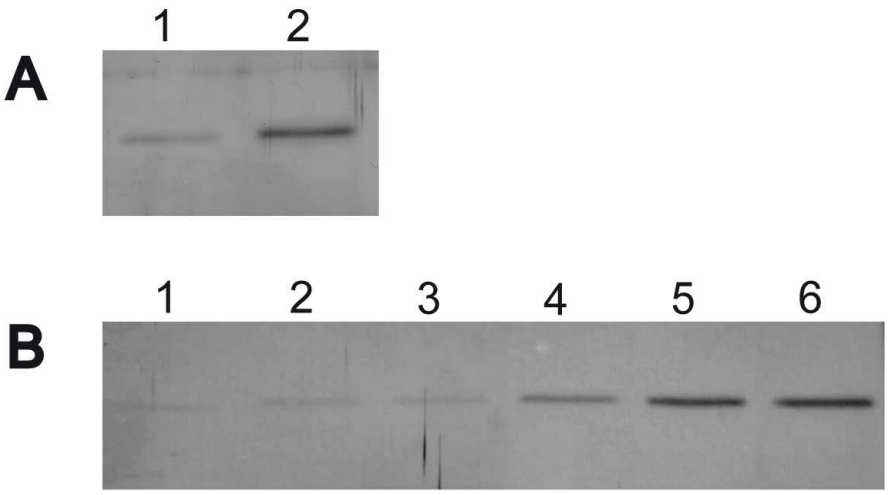

Figure 5

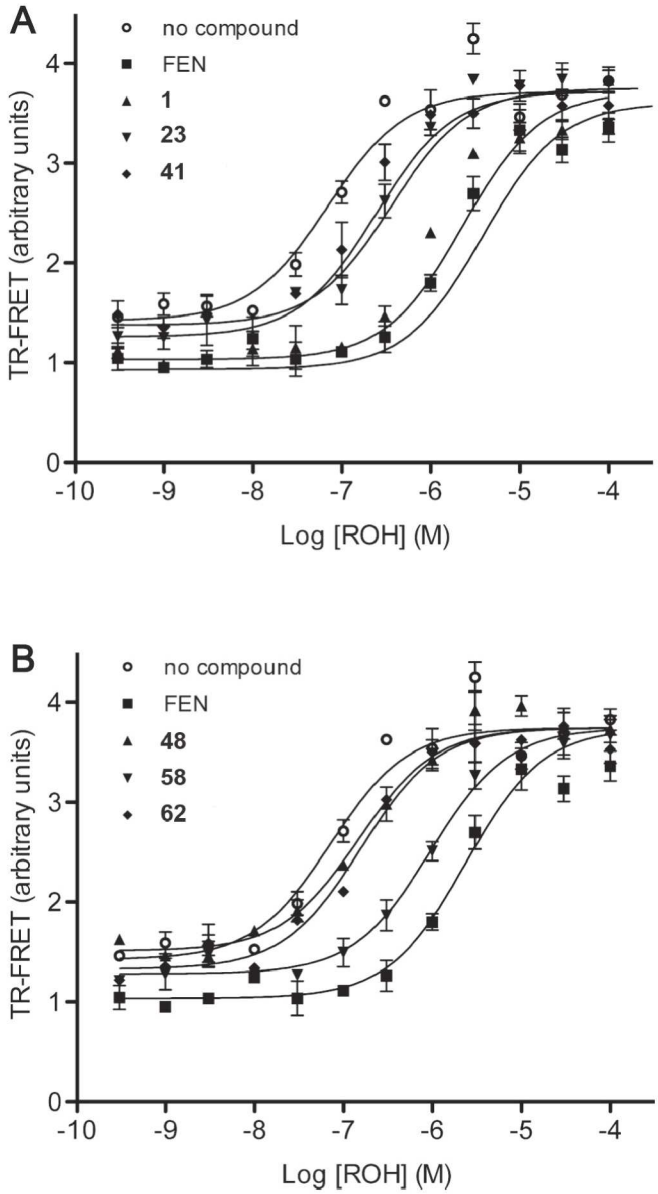
A
no compound
FEN
1
23
41
TR-FRET (arbitrary units)
Log [ROH] (M)
B
no compound
FEN
48
58
62
TR-FRET (arbitrary units)
Log [ROH] (M)

Figure 6

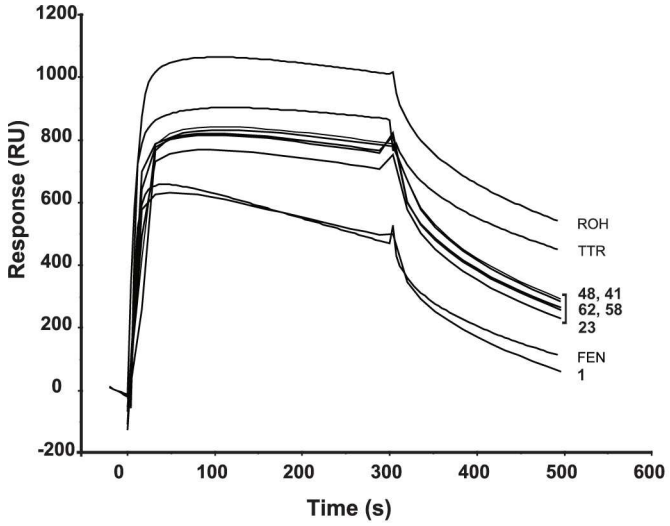
1200
1000
800
600
400
200
0
-200
Response (RU)
0
100
200
300
400
500
600
Time (s)
ROH
TTR
48, 41
62, 58
23
FEN
1

Figure 7

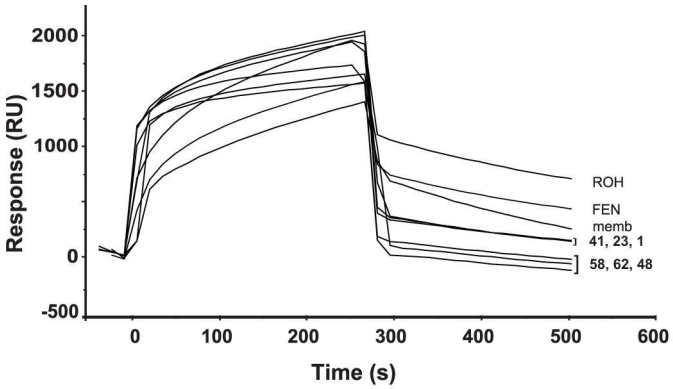
2000
1500
1000
0
-500
Response (RU)
0
100
200
300
400
500
600
Time (s)
ROH
FEN
memb
41, 23, 1
58, 62, 48

Figure Captions:

Figure 1: Figure A: three dimensional (3D) image of ROH (in blue) in sRBP (PDB: 1RBP[4]) and FEN (in yellow) in sRBP (PDB: 1FEL[16]) with contacting residues labelled and illustrated in stick format. Images have been provided at a six degree rotation around the y axis. Images produced using Pymol.[39] Figures B & C: 2D depiction of ROH and FEN binding poses as depicted using MOE.[20] Figure D: caption indicating the 2D interactions in the binding pose as depicted using MOE.

Figure 2. 2D image of Fenretinide (FEN), which differs from ROH by a phenylamide in place of the hydroxyl group. **A**: depicts the area where the variations were introduced at the β-ionone ring end of FEN – compounds **2-22**. **B**: depicts the polyene end of FEN where variations were introduced – compounds **1** and **23-68**.

Figure 3: Titration of apo-sRBP with a selection of compounds. For quenching of the protein fluorescence the excitation and emission wavelengths were 280 nm and 345 nm, respectively. The titration system consisted of 0.5 mL of 2 μM of the purified apo-sRBP in PBS, pH 7.4. Solutions of ROH, FEN or compounds in ethanol were added to the cuvette until a concentration of 7.5 μM. The curves shown were corrected for inner filter effect of the compounds.

Figure 4: Pull-down assay for sRBP after incubation with compounds**. A:** the ROH-sRBP-HisTTR complex was incubated in the presence of 10 μM ROH and 100 μM FEN. After incubation the complexes and free sRBP were separated by pull-down and the

flow-throughs analyzed by SDS-PAGE. Lanes reveal free sRBP in the flow-through fractions. Lane 1: control (10 μM ROH, no compound); lane 2: 10 μM retinol + 100μM FEN (positive control for complex disruption). **B:** Dose-response pull-down assay for **58**. Lane 1: control (10 μM ROH, no compound); remaining lanes contain 10 μM ROH + different concentrations of **58** (1, 10, 20, 50 and 100 μM, respectively).

Figure 5: Time-resolved FRET for the sRBP-TTR interaction. Assays were conducted with a fixed concentration (10 μM) of compound and increasing concentrations of ROH. sRBP and TTR concentrations were 5 and 100 nM, respectively. TR-FRET signals are the ratios between 665 nm and 615 nm emissions. The curves were generated using a sigmoidal dose-response equation in Prism GraphPad Software Inc.). Results shown are from a representative experiment performed in duplicates ± standard deviations.

Figure 6: Sensorgram showing His-sRBP interactions with TTR in the presence of selected compounds. SPR response curves reflect the interaction of TTR with immobilized sRBP. The responses were recorded as a function of time and are expressed in resonance units (RU).

Figure 7: Sensorgram showing His-sRBP interactions with solubilised HEK293 cell membranes in the presence of selected compounds. SPR response curves reflect the interaction of HEK293 cell solubilised membrane preparations flown over immobilized

sRBP. The responses were recorded as a function of time and are expressed in resonance units (RU).

Table of Contents Graphic

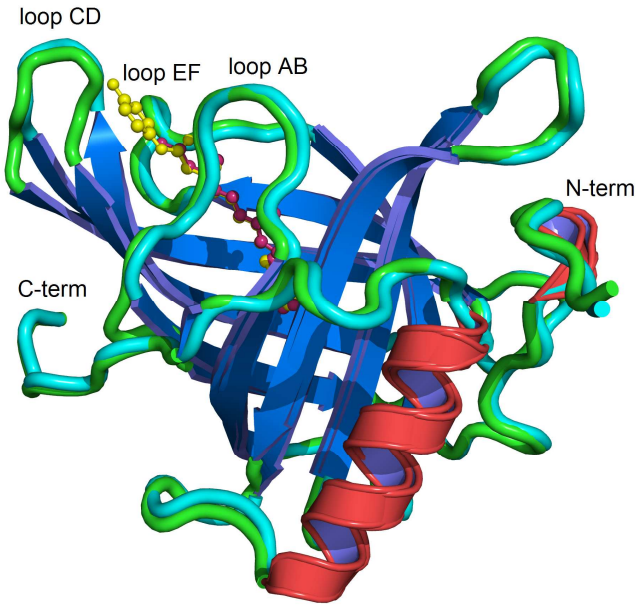

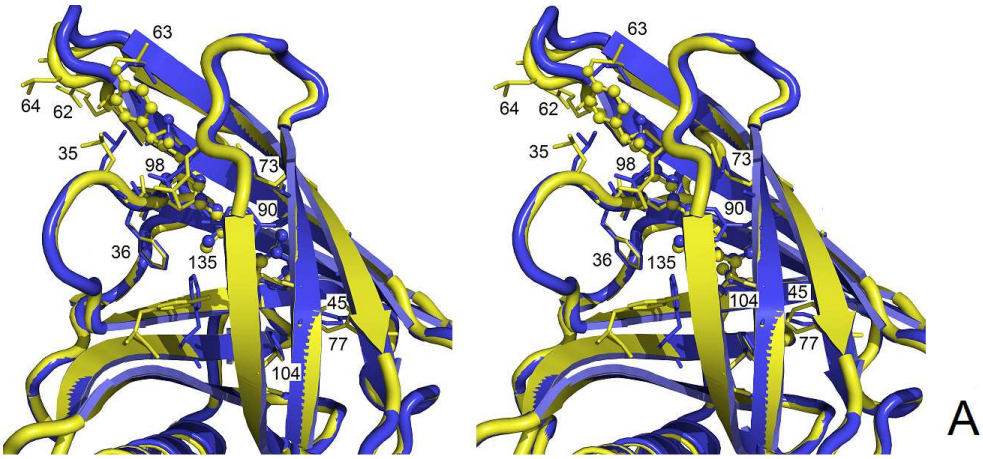

Figure 1: Figure A: three dimensional (3D) image of ROH (in blue) in sRBP (PDB: 1RBP4) and FEN (in yellow) in sRBP (PDB: 1FEL16) with contacting residues labelled and illustrated in stick format. Images have been provided at a six degree rotation around the y axis. Images produced using Pymol.39 Figures B & C: 2D depiction of ROH and FEN binding poses as depicted using MOE.20 Figure D: caption indicating the 2D interactions in the binding pose as depicted using MOE.
352x159mm (96 x 96 DPI)

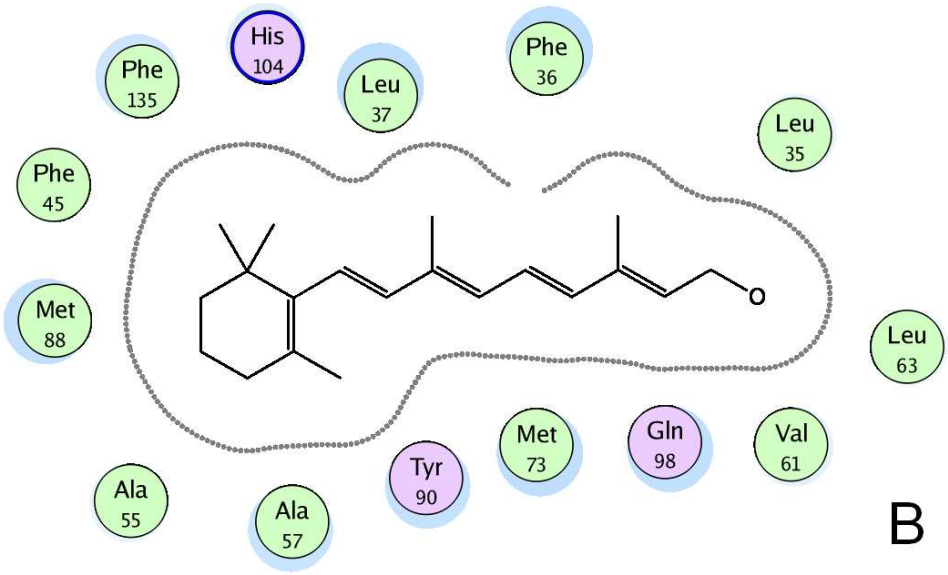

290x180mm (96 x 96 DPI)

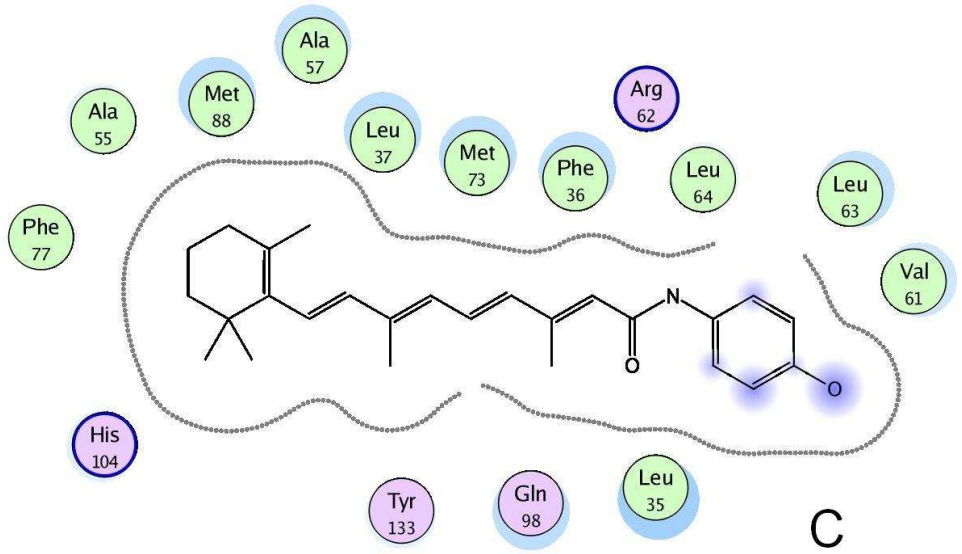

328x193mm (96 x 96 DPI)

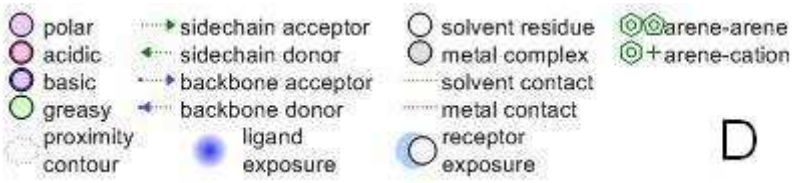

115x25mm (96 x 96 DPI)

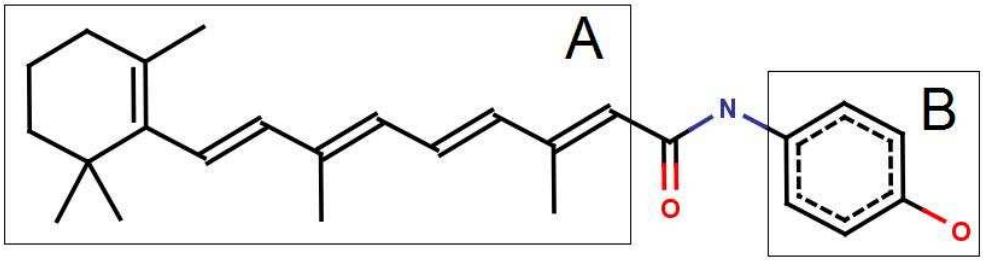

2D image of Fenretinide (FEN), which differs from ROH by a phenylamide in place of the hydroxyl group. A: depicts the area where the variations were introduced at the β-ionone ring end of FEN – compounds 2-22. B: depicts the polyene end of FEN where variations were introduced – compounds 1 and 23-68.
219x62mm (96 x 96 DPI)

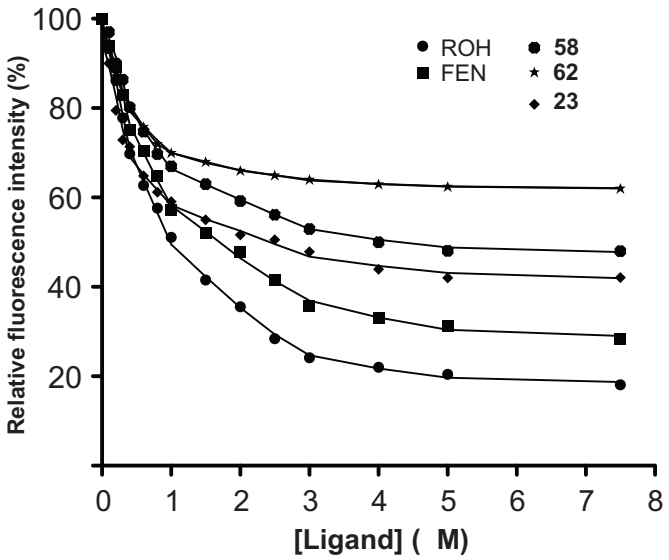
100
80
60
40
20
Relative fluorescence intensity (%)
ROH
FEN
58
62
23
0
1
2
3
4
5
6
7
8
[Ligand] (M)

Figure 3

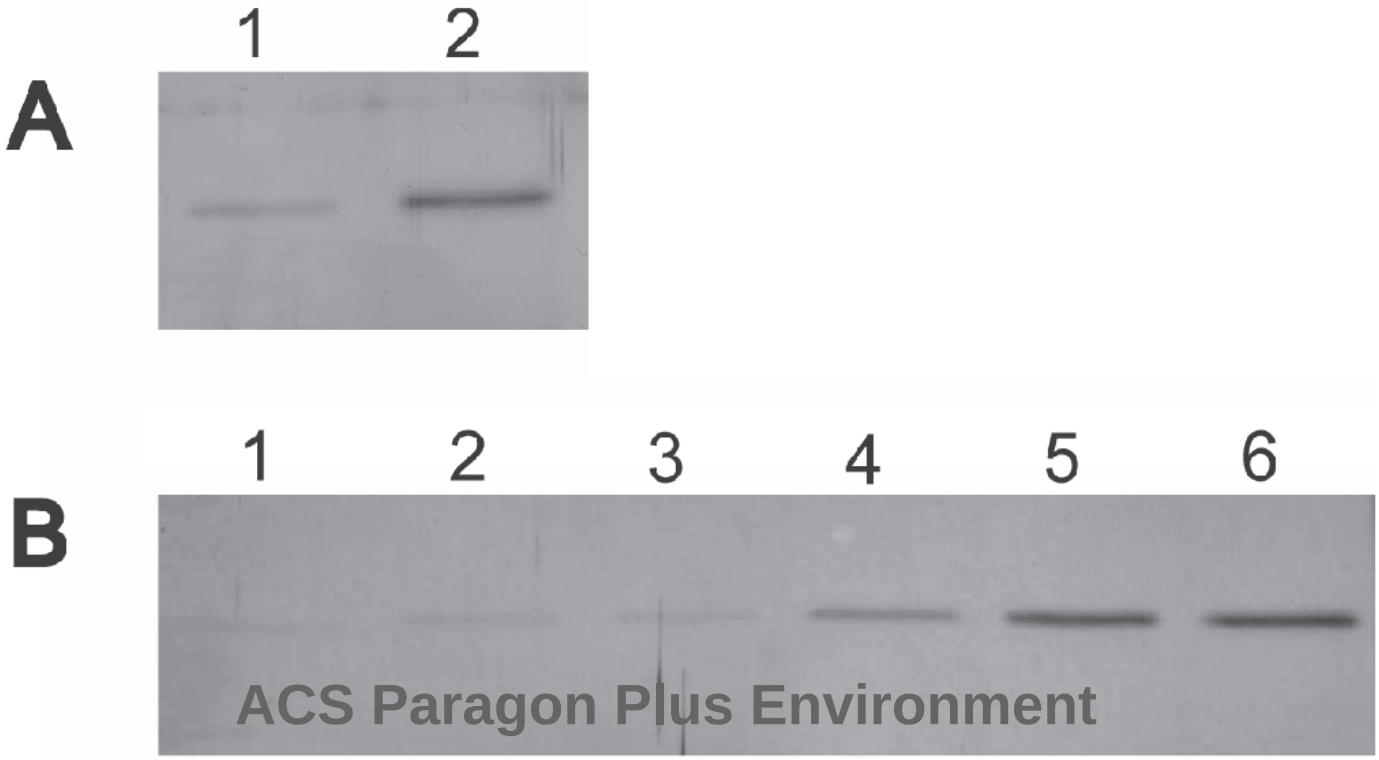

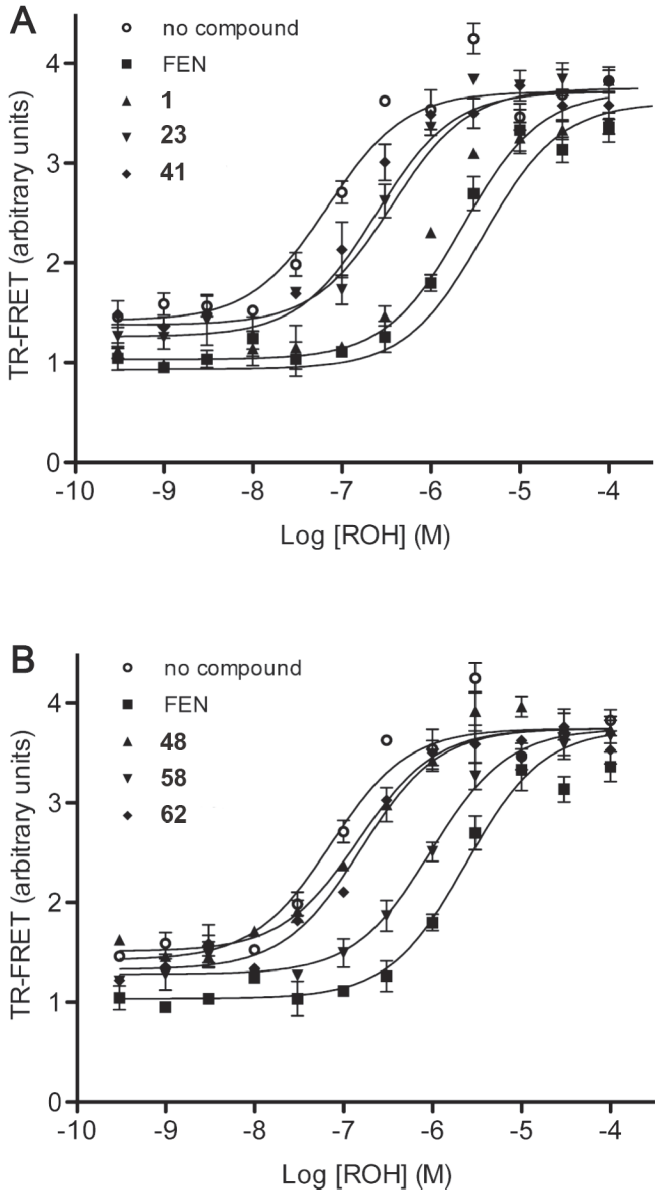
A
no compound
FEN
1
23
41
TR-FRET (arbitrary units)
Log [ROH] (M)
B
no compound
FEN
48
58
62
TR-FRET (arbitrary units)
Log [ROH] (M)

Figure 5

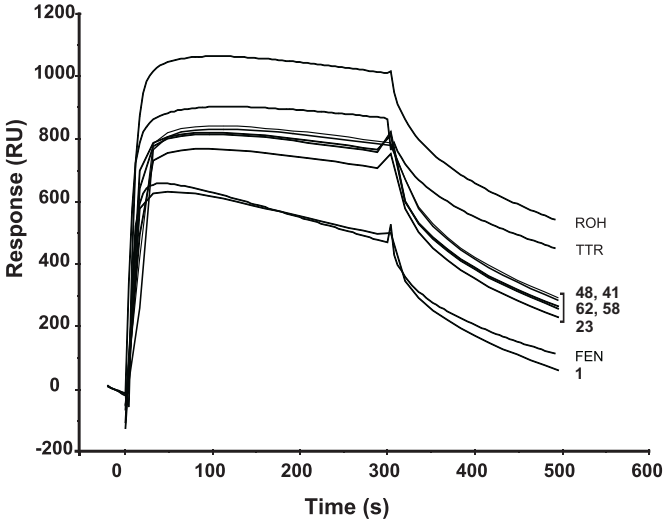
1200
1000
800
600
400
200
0
-200
Response (RU)
0
100
200
300
400
500
600
Time (s)
ROH
TTR
48, 41
62, 58
23
FEN
1

Figure 6

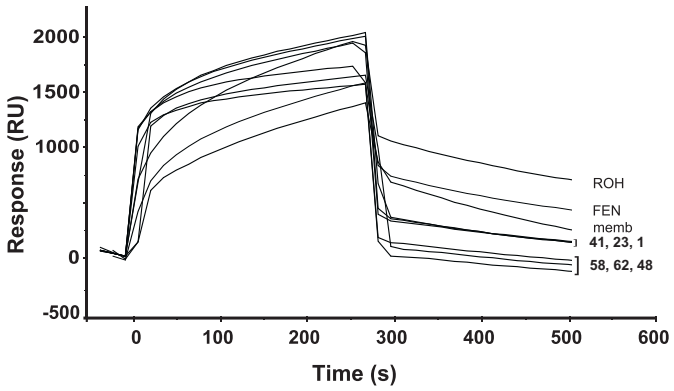
2000
1500
1000
0
-500
Response (RU)
0
100
200
300
400
500
600
Time (s)
ROH
FEN
memb
41, 23, 1
58, 62, 48

Figure7

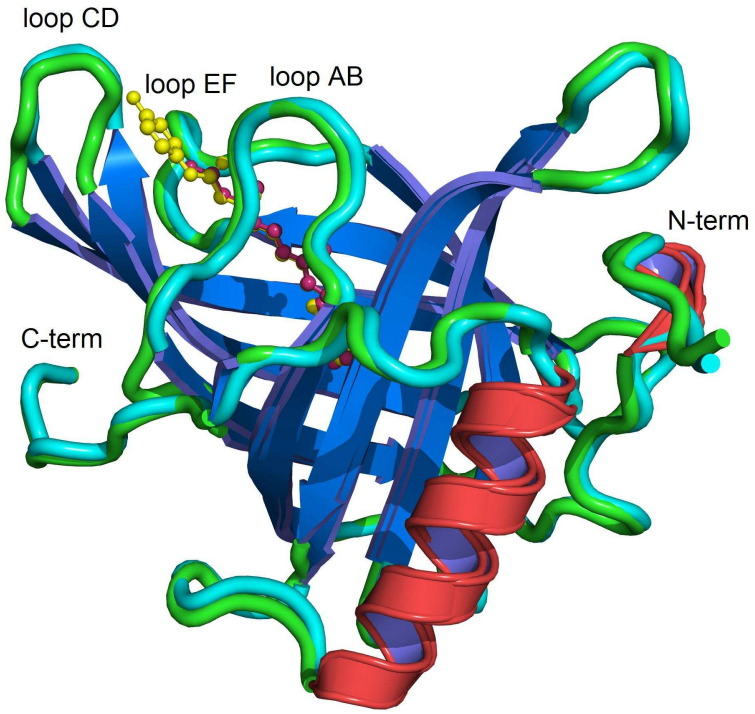

Superimposed image of Retinol (ROH in pink) and Fenretinide (FEN in yellow) in sRBP (PDB: 1RBP and 1FEL).
635x635mm (96 x 96 DPI)